International Journal of Engineering Research & Technology (IJERT)
ISSN: 2278-0181
Vol. 3 Issue 6, June - 2014

Enhanced Performance of a Frequency Up-Converted Piezoelectric Energy Harvester for Wideband Vibration

Miah A. Halim, Jae Y. Park
Department of Electronic Engineering, Kwangwoon University,
447-1, Wolgye-dong, Nowon-gu, Seoul 139-701, South Korea

***Abstract*— This paper demonstrates enhanced performance of a mechanical impact driven frequency up-converted piezoelectric vibration energy harvester to scavenge energy from a wide range of low frequency ambient vibration. Increased bandwidth of the harvester has been obtained by increasing the stiffness of its power generating elements. The harvester structure comprises a low-frequency flexible driving beam with laterally expanded rectangular tip mass and two high-frequency unimorph piezoelectric generating beams which are struck by the driving beam mass upon excitation, and generate power. This impact mechanism results in a hindrance of the vibration motion of the driving beam, and its frequency response diverges from normal behavior, introducing wideband operation. Increase in generating beams' stiffness causes an increase in the effective stiffness of driving beam after impact which, in turn, allows bandwidth enhancement. Two different sets of unimorph generating beams have been used. Among those, use of relatively stiffer beams, made of stainless steel support layer, offers 60% increased half-power bandwidth (8Hz) and almost 3 times increased peak power (377μW) than the other, made of styrene support layer. It generates significant power within the entire operating frequency range (6Hz to 15Hz) implying its potential to be implemented in human and machine motion applications.**

Keywords*— *Effective stiffness; Unimorph beam; Frequency up-conversion; Mechanical impact; Wide bandwidth; Ambient vibration

I. INTRODUCTION

With the recent advances in wireless and micro-electromechanical system (MEMS) technology, energy harvesting becomes one of the most promising technologies as the alternatives of the conventional batteries. The life of a battery is limited and short compared to the working life of any portable electronics and wireless devices. Sometimes it is inefficient to replace or recharge battery. Therefore, a good number of researchers have been investigating since past few years for the energy harvesting technology as a self-power source of these portable electronics and wireless devices. Ambient vibration is one of the most common and versatile energy sources around our environment [1]. Energy harvesting from ambient vibration is a clean and regenerative means of powering small-scale systems. Vibration energy is typically converted into electrical energy using electrostatic, piezoelectric, electromagnetic, or magnetoelectric transduction mechanisms [2-5]. A vibration energy harvester typically employs spring-mass-damper system having a resonant frequency at which the output voltage or power is maximum and significantly drops at other frequencies. In order to achieve maximum power from a vibration energy harvester, the frequency of vibration must match its resonant frequency.

Ambient vibrations around our environment are characterized by low frequencies (<10Hz for human motion and <100Hz for machine induced motion) having capricious nature with high amplitudes [6]. Energy harvesting from such low frequency vibrations is challenging because— (i) different vibration sources produce vibration of different frequencies containing various cyclic movements in different directions which does not allow the resonant oscillator to respond at it resonant frequency [7]; (ii) a low frequency resonator consists of a large mass combined with a compliant spring that undergoes large oscillation even at low level acceleration (<1g) making the harvesting device large for any specific application [8]; (iii) average power flow decreases with the decrease in resonant frequency as the generated power is directly proportional to the cube of the frequency of vibration [9]; (iv) it requires a relatively high electromechanical coupling [10]. Thus, it is quite difficult to produce significant amount of power from low frequency ambient vibration. In order to meet the challenges aforementioned, researchers have reported frequency up-conversion mechanism in low frequency vibration energy harvesting. In a frequency up-converted energy harvester, a low frequency oscillator absorbs the kinetic energy from the ambient vibration and transfers it to one or more high frequency oscillators either by mechanical impact or by magnetic attraction/repulsion which convert the kinetic energy to electrical energy. Impact driven frequency up-converted energy harvesters have been reported in [11-14] whereas those with magnetic attraction/repulsion have been reported in [15-18]. However, reported frequency up-converted harvesters still have the limitations in operating within a wide range of low frequency vibrations which have the random movements in nature (particularly, vibrations below 20 Hz), desiring a wideband operation.

In this study, we have presented enhancement of both bandwidth and output power of a low frequency driven piezoelectric vibration energy harvester that uses frequency up-conversion of two piezoelectric generating beams by mechanical impact of a mass-loaded flexible driving beam. The generating beams act as one single flexible stopper to the driving beam. The effective stiffness of the driving beam increases after impact on the rigid generating beams,

introducing its non-linear vibration that allows the system to operate within a wider frequency range. Each of the stiffer generating beams among two different sets of generating beams, generates the maximum allowable power over almost entire operating bandwidth (half-power bandwidth) which are (both generated power and operating bandwidth) significantly higher than the relatively less stiff generating beams set.

II. SYSTEM DESIGN AND MODELING

A. Wideband Operation by Mechanical Impact

Fig. 1 illustrates the concept of bandwidth widening by mechanical impact. Generally, when a mass-loaded cantilever beam vibrates freely (no stopper), the stiffness of the beam is constant over its displacement and it shows linear frequency response behavior. But, involvement of any obstruction (stopper) on its way of motion, the vibration motion of the mass-loaded cantilever beam is hampered due to impact on the stopper that changes its effective stiffness and the frequency response diverges from its normal behavior. Fig. 1(a) shows the schematic of an impact model that contains one proof-mass-loaded driving cantilever beam of stiffness k_1 and a generating cantilever beam of stiffness k_2, ($k_1 << k_2$) placed below with a small gap d, acting as a stopper to the driving beam. When vibration with sufficient large amplitude is applied, the mass impacts on the generating beam stopper. As the generating beam mass is negligible as compared to the proof-mass m, both beams vibrate together after impact for a short period (coupled vibration) and then vibrate independently (free vibration) after separation. The coupled vibration changes the effective stiffness of the driving beam to (k_1+k_2) as shown in Fig. 1(b), introducing its non-linear vibration, allowing resonance to extend over a wider interval, in the vicinity of the it's resonant frequency as shown in Fig. 1(c). This system can be modeled as a single degree of freedom (SDOF) piecewise linear model [19] as shown in Fig. 1(d).

B. Proposed Device Structure and Its Working

The structure of the proposed impact based wideband energy harvester has been illustrated in Fig. 2. It consists of a proof-mass loaded flexible driving beam having lower stiffness and two similar type rigid generating beams having higher stiffness than the driving beam as shown in Fig. 2(a). The generating beams are placed below the driving beam at the same level with a small gap as shown in Fig. 2(b). The driving beam has a laterally expanded tip at which a rectangular proof-mass (fitted to the expanded tip) is attached whereas each generating beam is composed of a piezoelectric layer mounted over a non-piezoelectric support layer as shown in Fig. 2(c). As seen, two different sets of generating beams with different support layers (*Type-1* and *Type-2*) have been used in order to compare the performance. *Type-2* beams are more rigid than *Type-1* beams. Moreover, the length ratio of piezoelectric and non-piezoelectric layers are different for two beam types. Details of beam geometry will be discussed in the prototype fabrication section.

When a low frequency external vibration of sufficiently large amplitude is applied to the harvester, the flexible driving beam starts vibrating and the proof-mass impacts on two rigid generating beams periodically. After impact, both driving and generating beams vibrate together for a short period with system's coupled vibration frequency and then separate. After separation, each generating beam vibrates freely with its own resonant frequency which introduces frequency up-conversion mechanism. The piezoelectric layer of each generating beam generates electricity due to the piezoelectric effect.

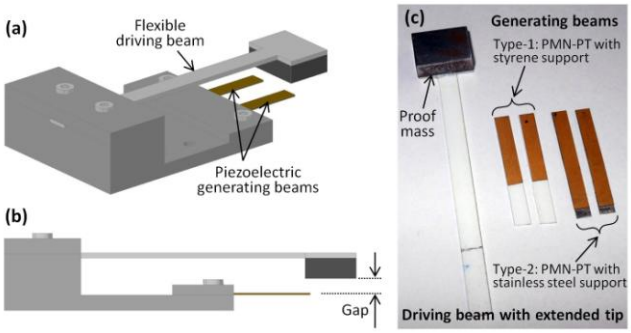

Fig. 2: Structure of the proposed energy harvester: (a) schematic drawing, (b) side view, and (c) photographs of driving and generating beams.

C. Electromechanical Modeling

According to the piecewise linear model, the impact behavior of the proposed system is similar to an inelastic collision because the effective mass of each generating beam is negligible as compared to that of the proof-mass attached to the driving beam tip [11]. When the system is externally excited by a harmonic acceleration a, it allows the proof-mass to move relative to the base as z. If $z < d$, then there is no impact on the generating beams. Only the mass-loaded driving beam vibrates independently. If $z \geq d$ (while excited with sufficient large acceleration), the proof-mass impacts on the generating beams. They stick and vibrate together for a short period with an increased stiffness (k_1+2k_2) which transforms the proof-mass motion from linear to non-linear. This enables the resonance of the driving beam to extend over a wider frequency range [19]. The tendency of non-linearity in driving beam motion increases as the effective stiffness during coupled vibration period increases which, in turn, enhances the bandwidth significantly. Therefore, the piecewise linear equation of driving beam motion can be expressed as

$$m\ddot{z} + c_1\dot{z} + k_1 z = ma\sin(\omega_a t); \qquad z < d \tag{1a}$$

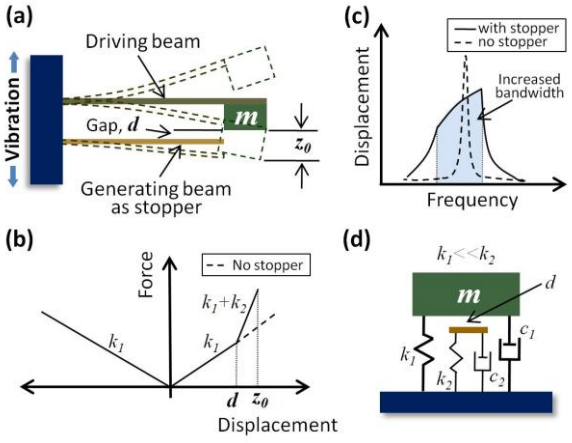

Fig. 1: Concept of bandwidth widening by impact: (a) schematic view, (b) typical stiffness variation, (c) typical frequency response, and (d) SDOF piecewise linear model.

$$m\ddot{z} + (c_1 + 2c_2)\dot{z} + (k_1 + 2k_2)z - 2k_2 d = ma\sin(\omega_a t); \qquad z \geq d \qquad (1b)$$

where c_1 and c_2 are the damping constants of driving beam and each generating beam, respectively. ω_a is the frequency of applied excitation. Since the coupled vibration period is over, the proof mass moves away from the generating beams and each generating beam vibrates at its own resonant frequency with exponentially decayed amplitude, while the driving beam reverts to its original linear motion behavior until it impacts the generating beams during the next cycle. It is assumed that the vibration of each generating beam decays fully and stays at position *d*, before the next impact cycle approaching.

Let us consider, each unimorph generating beam of effective length L and width w has a piezoelectric layer of thickness t_p and a non-piezoelectric support layer of thickness t_s. When an impact force F_{imp} is applied at the tip by the driving beam proof-mass, the average stress on the surface of the piezoelectric layer can be given as [20]

$$\sigma = \frac{F_{imp} E_p}{wD}\left(t_n t_p + \frac{1}{2}t_p^2\right) \qquad (2)$$

in which E_p is the Young's modulus of the piezoelectric layer, D is the bending modulus per unit width of the beam and t_n is the position of the neutral plane from the bonding plane. Therefore, the generated open circuit voltage can be expressed in terms of average stress and the material properties of the piezoelectric layer, such as

$$V_{OC} = \frac{1}{2}L\left(\frac{-d_{31}}{\varepsilon_r \varepsilon_0}\right)\frac{F_{imp} E_p}{wD}\left(t_n t_p + \frac{1}{2}t_p^2\right) \qquad (3)$$

where $-d_{31}$ is the piezoelectric strain constant, ε_r and ε_0 are the dielectric constant of the piezoelectric layer and the permittivity of free space, respectively. According to the piecewise linear dynamics of the periodic impact vibration model described earlier, the instantaneous output voltage of each generating beam connected to a matched load as a function of time t can be written as [12]

$$V(t) = \begin{cases} \frac{V_{OC}}{4} e^{-\zeta_T \omega_c t}\sin(\omega_c t); & n\frac{2\pi}{\omega_a} \leq t \leq (n+1)\frac{3\pi}{2\omega_c} \\ \frac{V_{OC}}{4} e^{-\zeta_T \omega_g t}\sin\left(\omega_g\left(t + \frac{3\pi}{2}\right)\right); & (n+1)\frac{3\pi}{2\omega_c} \leq t \leq (n+1)\frac{2\pi}{\omega_a} \end{cases} \qquad (4)$$

where n = 0,1,2,3,..... is the number of impact, ζ_T is the total (sum of mechanical and electrical) damping ratio, ω_g is the resonant frequency of each generating beam, and ω_c is the frequency of the coupled vibration which can be calculated assuming that the driving beam mass and the generating beams never separate after impact, as $\omega_c = \sqrt{(k_1 + 2k_2)/m}$. The peak power, generated from each generating beam, delivered to load can be written as

$$P_{peak} = \frac{V_{OC}^2 R_L}{(R_S + R_L)^2} \qquad (5)$$

When the applied load resistance R_L matches the source resistance R_S, then maximum power is achieved. The source resistance is estimated as $R_S = 1/(\omega_r C)$, where ω_r (= ω_g) is the resonant frequency and C is the capacitance of the piezoelectric layer.

TABLE I: MATERIAL PARAMETERS AND GEOMETRY OF THE PROPOSED ENERGY HARVESTER

Parameter	Driving Beam	Generating Beam	
		Type-1	*Type-2*
Effective length of the beam	55 mm	15 mm	15 mm
Width of the beam	4.8 mm	3.5 mm	3.5 mm
Thickness of the beam	1 mm	0.8 mm	0.4 mm
Length of piezoelectric layer	-	15 mm	25 mm
Thickness of piezoelectric layer	-	0.3 mm	0.3 mm
Support layer thickness	-	0.5 mm	0.1 mm
Proof-mass	4.36 gm	-	-
Young's modulus of styrene	3 GPa	3 GPa	-
Young's modulus of stainless steel	-	-	200 GPa
Young's modulus of PMN-PT*	-	20 GPa	20 GPa
Dielectric constant of PMN-PT*	-	5200	5200
Piezoelectric strain coefficient*	-	2000 pC/N	2000 pC/N
Capacitance of PMN-PT*	-	9.85 nF	13.5 nF

*Piezoelectric (PMN-PT) material parameters were provided by the supplier.

III. PROTOTYPE FABRICATION

In order to verify the performance of the proposed energy harvester, a macro prototype was assembled on an Aluminum base structure. The driving beam was made of a flexible styrene strip with laterally expanded tip of area 14×10 mm^2. An iron (Fe) proof-mass was attached with the driving beam tip to lessen its resonant frequency. Four generating beams were prepared. Two of those (*Type-1*) were made by mounting PMN-PT single crystal piezoelectric layers with gold (Au) electrodes (supplied by Ibule Photonics, South Korea) on the styrene strip support layers by silver epoxy (Eccobond 56CJ; Emerson & Cuming). Another two (*Type-2*) were made of stainless steel support layers in the similar way. The clamp area of *Type-1* generating beam was not covered with piezoelectric layer; length of piezoelectric layer was equal to the effective length of the generating beam. Two similar type generating beams (either *Type*-1 or *Type-2*) were placed at both sides of the driving beam, below it, 7 mm apart, at the same level so that the proof-mass attached to the laterally expanded driving beam tip can impact on both generating beams' free ends at the same time, during its vibration. The vertical gap between the proof-mass and both generating beams was kept so small (in this case, 0.5 mm) that the mass can impact on the generating beams' free ends within its displacement over an interesting frequency range. However, the gap should not be zero because the higher resonant

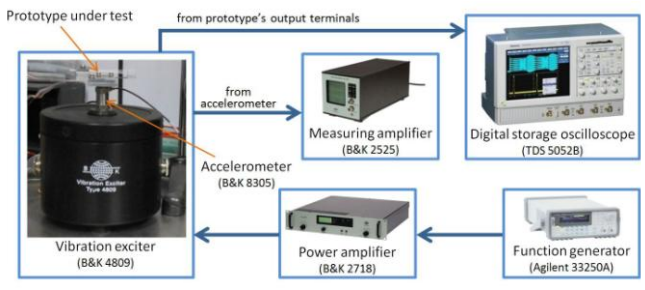

Fig. 3: Schematic of experimental setup and photographs of the prototype energy harvester under vibration exciter test.

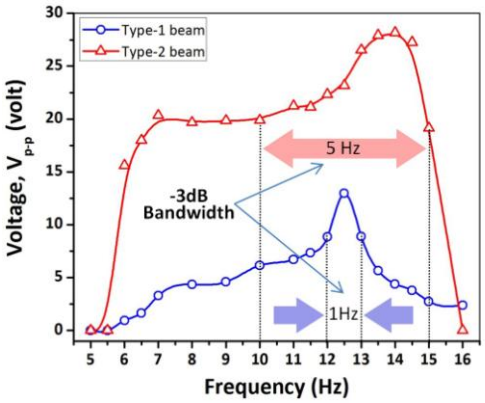

Fig. 4: Measured open circuit voltage of one single generating beam of *Type-1* and *Type-2* under 6 ms-2 acceleration within low frequency range.

frequency of the coupled vibration limits the driving beams' ability to respond to a lower frequency excitation at typical acceleration amplitudes. Table I presents the material parameters and geometry of the proposed energy harvester.

IV. EXPERIMENTAL RESULTS AND DISCUSSION

A. *Experimental Setup*

We measured the performances of the fabricated energy harvester with two different types (*Type-1* and *Type-2*) of generating beams in order to prove the concept of enhancing bandwidth by impact under low frequency vibration. Fig. 3 illustrates the schematic of the complete experimental setup and the photograph of the fabricated prototype under test. The fabricated energy harvester prototype was mounted on a vibration exciter (B&K 4809) connected to a function generator (Agilent 33250A) in conjunction with a power amplifier (B&K 2718) which provides sinusoidal excitation of various frequencies and accelerations to the harvester prototype. The amplitude of the input vibration was measured by using a reference accelerometer (B&K 8305) attached to the base of the vibration exciter along with the harvester prototype, connected to a measuring amplifier (B&K 2525). A digital storage oscilloscope (Tektronix TDS5052B) was connected to the harvester outputs to measure and record its output response.

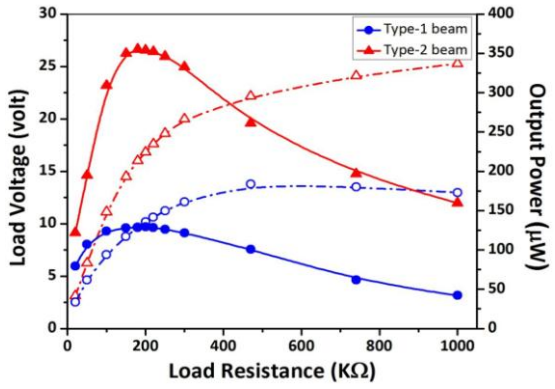

Fig. 5: Measured peak-peak load voltages (dashed lines) and peak output powers (solid lines) against various load resistances generated by one single generating beam of *Type-1* and *Type-2* at 12.5 Hz frequency under 6ms^{-2} acceleration.

B. *Results and Discussion*

Frequency response of the device was carried out by sweeping the applied vibration frequency from 5 Hz to 16 Hz, keeping the acceleration fixed at 6 ms^{-2}. Fig. 4 shows the generated peak-peak open circuit voltages of one single generating beam of *Type-1* and *Type-2*. A maximum 12.96 volt was obtained at 12.5 Hz resonant frequency from *Type-1* beam while *Type-2* beam generated maximum 28.16 volt at 14 Hz resonant frequency. The higher stiffness of *Type-2* generating beam produces larger strain on the Piezoelectric layer during impact, resulting in higher output voltage. The impact results in a hindrance of the vibration motion in driving beam, and the frequency response diverges from its normal behavior enabling the resonance to extend over a wide range. The resonant peak shifts slightly towards higher frequency for *Type-2* beam due to increased effective stiffness of the driving beam during coupled vibration after impact which, in turn, increases the -3dB bandwidth (5 Hz) as compared to that (1 Hz) of *Type-1* beam.

Fig. 5 plots the measured peak-peak output voltage across various load resistances and the peak power delivered to the load at 12.5 Hz, under 6 ms^{-2} acceleration. Results show that, a maximum peak power of 129.15 μW was delivered to a matched load resistance of 200 KΩ from each *Type-1* generating beam. On the other hand, each *Type-2* beam delivered a maximum 355μW peak power to 180 KΩ optimal load. This optimal load resistance values match the frequency of the coupled vibration of the driving and generating beams rather than that of the free vibration of the generating beam, because most of the output was obtained during the coupled vibration. The values of peak power were calculated by $V_L^2/4R_L$; where V_L is the peak-peak voltage across the load resistance R_L.

The characteristics of instantaneous voltage waveforms generated by *Type-1* and *Type-2* beams are shown in Fig. 6. They show similar characteristics. The generated voltage amplitude decays exponentially with time as predicted but not perfectly exponential because of imperfect bonding of piezoelectric layer with the support layer. It is almost zero over half of the cycle because of the longer time interval between two consecutive impacts. It can be minimized by reducing the time interval between two consecutive impacts by applying multiple impacts during a single cycle of the

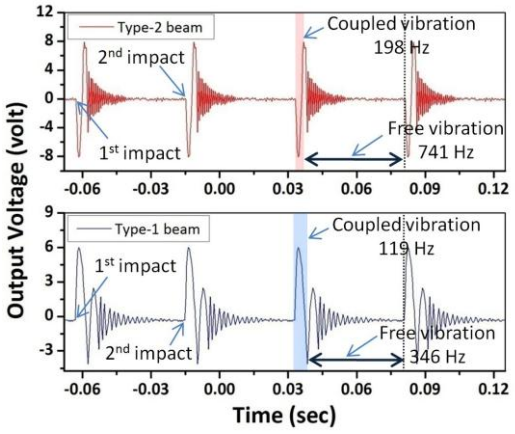

Fig. 6: Instantaneous output voltage waveforms generated by one *Type-1* (bottom) and one *Type-2* (top) generating beams across respective optimum load resistances at 12.5 Hz frequency under 6 ms^{-2} acceleration.

TABLE II: DAMPING RATIO, Q-FACTOR AND ENERGY CONVERSION EFFICIENCY OF THE DEVICE

Parameter	Device with.....	
	Type-1 beams	*Type-2 beams*
Mechanical damping ratio, ζ_m	0.013	0.018
Total damping ratio, ζ_T	0.072	0.116
Electrical damping ratio, ζ_e	0.059	0.098
Mechanical Q-factor, Q	38.46	27.78
Energy conversion efficiency, η	81.9%	84.5%

driving beam vibration. Each highest peak corresponds to an impact between the proof-mass of the driving beam tip and the generating beams. By using Fast Fourier Transform (FFT), it has been observed that the frequencies of the system's coupled vibration and free vibration of the generating beam were 119 Hz and 346 Hz, respectively for *Type-1* beam and, 198 Hz and 731 Hz, respectively for *Type-2* beam. This clearly illustrates the frequency up-conversion behavior of the device even though the applied frequency was 12.5 Hz.

In order to determine the mechanical Quality factor, Q and energy conversion efficiency, η of the proposed system, we measured the damping ratio (both mechanical and electrical) by flick test which are related as [8, 21]

$$Q = \frac{1}{2\zeta_m} \tag{6}$$

$$\eta = \frac{\zeta_e}{(\zeta_m + \zeta_e)} \times 100\% \tag{7}$$

where ζ_m and ζ_e are the mechanical and electrical damping ratio, respectively. Flick test was done by applying a high amplitude impulse (pulse period 30ms, pulse width 500µs, and acceleration amplitude 30.3 ms^{-2}) to the generating beams and monitoring the decay of the generated output voltage amplitude over time without and with load to the terminals. The corresponding damping ratio, then, be calculated from the decay plot using the following relationship

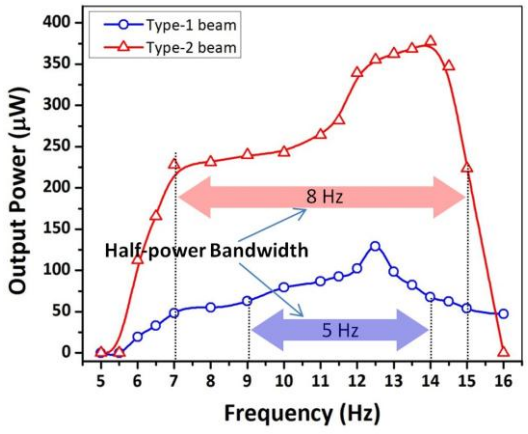

Fig. 7: Measured peak output powers delivered to respective optimum load resistances of one single *Type-1* and *Type-2* generating beams against applied frequency under 6ms^{-2} accelerations.

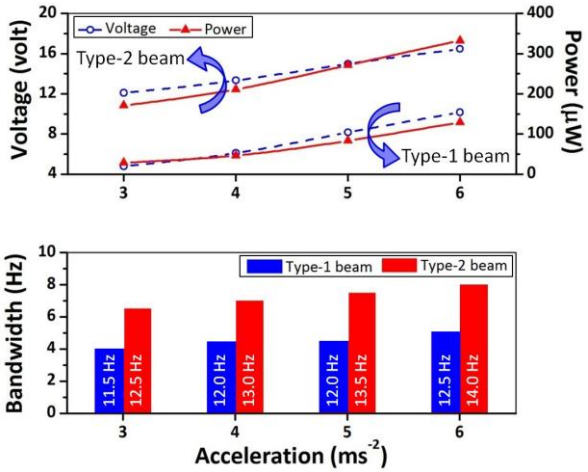

Fig. 8: Comparison of different output responses of the device with *Type-1* and *Type-2* generating beams measured at different accelerations.

$$\zeta = \frac{\ln(a_1/a_2)}{\sqrt{4\pi^2 + [\ln(a_1/a_2)]^2}} \tag{8}$$

where a_1 and a_2 are the consecutive peak amplitudes in the plot. A number of impulse responses were recorded and an average value of the damping ratio was taken. Open circuit impulse response (without load) gives the mechanical damping ratio ζ_m whereas load connected impulse response gives the total damping ratio ζ_T. Electrical damping ratio ζ_e was obtained as $\zeta_e = (\zeta_T - \zeta_m)$. Table II summarizes the values of damping ratio, Q-factor and energy conversion efficiency of the device with *Type-1* and *Type-2* generating beams.

Fig. 7 shows the peak output powers delivered from one generating beam to the respective optimal load resistances of the device with *Type-1* and *Type-2* beams against operating frequencies at 6 ms^{-2} acceleration. A maximum peak power of 129.15 µW was delivered by *Type-1* beam at 12.5 Hz while *Type-2* beam generated maximum 377.21 µW peak power at 14 Hz frequency. In case of *Type-2* beam, the resonant peak shifts slightly towards higher frequency (as also seen in the frequency response curve) because increased effective stiffness of the driving beam which also introduces increased half-power bandwidth. The half-power bandwidth of the device with *Type-1* beams is 5 Hz (from 9 Hz to 14 Hz) and that with *Type-2* beams is 8 Hz (from 7 Hz to 15 Hz). The experimental results clearly shows that use of much rigid generating beam stoppers not only increases (2.92 times) the output power but also increases (60%) the half-power bandwidth than relatively less rigid generating beam stoppers. It is capable of generating significant power (more than 227 µW peak power) within 89% of its operating frequency range (from 6 Hz to 15 Hz). This has made the great innovation of our proposed impact based system in low frequency energy harvesting. Besides, use of two similar generating beams increases the power density of the device.

The output responses of the proposed device with two different sets of generating beam type were measured under various accelerations as illustrated in Fig. 8. As seen from the figure that voltage, power and half-power bandwidth increases with the increase in the acceleration for both types of beams. The impact force increases with the acceleration, resulting in increased stress on the PMN-PT surfaces which, in turn,

increases the output voltages and powers. Moreover, the resonant peaks slightly shifts towards higher frequency in both cases as the acceleration increases (indicated by vertical texts within the columns in the bottom graph). Higher impact force results in the retardation of the driving beams' vibration amplitude and increases the effective stiffness after impact. Higher effective stiffness increases the effective resonant frequency of the driving beam, enabling the resonance to enhance over a wide interval of the applied frequency spectrum.

V. CONCLUSIONS

Enhancement of operating bandwidth along with the output power of a mechanical impact driven frequency up-converted piezoelectric energy harvester has been investigated for improving the performance at very low ambient vibration frequencies. A macroscale prototype was fabricated by assembling a flexible driving beam with a proof-mass attached at its expanded tip that impacts on two piezoelectric generating beams at the same time, placed below it at the same level, while externally excited. Two different sets of generating beams were used to compare the performance of the device.. The device with stainless steel supported generating beams showed the improved performance than those with styrene support layers. It generates 2.92 times increased output power offering 60% increased half-power bandwidth (8 Hz) which is 89% of the operating frequency band (6 Hz to 15 Hz) of the proposed device. Results indicate the potential of the proposed idea to be implemented in harvesting energy from human and machine motion. There are still rooms for improving its output performances. Future work will include more optimized design and micro fabrication using MEMS process.

ACKNOWLEDGMENTS

The authors are grateful to acknowledge the support from the research grant of Kwangwoon University in 2014, the Basic Science Research Program (2013R1A1A2A10064810) and the Pioneer Research Centre Program (2010-0019313) through the National Research Foundation of Korea (NRF) funded by the Ministry of Science, ICT and Future Planning, Korea.

REFERENCES

[1] P. D. Mitcheson, E. M. Yeatman, G. K. Rao, A. S. Holmes, and T. C. Green, "Energy harvesting from human and machine motion for wireless electronic devices", Proc. IEEE, Vol. 96, No. 9, pp. 1457-1486, Sep. 2008.

[2] Y. Naruse, N. Matsubara, K. Mabuchi, M. Izumi, and S. Suzuki, "Electrostatic micro power generation from low frequency vibration such as human motion", J. Micromech. Microeng., Vol. 19, No. 9, pp. 094002, Sep. 2009.

[3] S. Saadon and O. Sidek, "A review of vibration based MEMS piezoelectric energy harvesters", Energy Convers. Manage., Vol. 52, No. 1, pp. 500-504, Jan. 2011.

[4] B. Yang, C. Lee, W. Xiang, J. Xie, J. H. He, R. K. Kotlanka, S. P. Low, and H. Feng, "Electromagnetic energy harvesting from vibrations of multiple frequencies", J. Micromech. Microeng., Vol. 19, No. 3, pp. 035001, Mar. 2009.

[5] X. Dai, Y. Wen, P. Li, J. Yang, and G. Zhang, "Modeling, characterization and fabrication of vibration energy harvester using Terfenol-D/PZT/Terfenol-D composite transducer", Sens. Actuators A: Physical, Vol. 156, No. 2, pp. 350-358, Dec. 2009.

[6] H. Külah and K. Najafi, "Energy scavenging from low-frequency vibrations by using frequency up-conversion for wireless sensor applications", IEEE Sens. J., Vol. 8, No. 3 pp. 261–268, Mar. 2008.

[7] A. R. M. Foisal , C. Hong and G.-S. Chung, "Multi-frequency electromagnetic energy harvester using a magnetic spring cantilever", Sens. Actuators A vol. 182, pp. 106-113, Aug. 2012.

[8] K. Ashraf, M. H. M. Khir, J. O. Dennis, and Z. Baharuddin, "Improved energy harvesting from low frequency vibrations by resonance amplification at multiple frequencies", Sens. Actuators A: Physical, Vol. 195, No. 1, pp. 123-132, Jun. 2013.

[9] C. B. Williams and R. B. Yates, "Analysis of micro-electric generator for microsystems", Sens. Actuators A: Physical, Vol. 52, No. 1-3, pp. 8-11, Mar.-Apr. 1996.

[10] N. G. Stephen, "On energy harvesting from ambient vibration", J. Sound Vib., Vol. 293, No. 1-2, pp. 409–425, May 2006.

[11] M. Renaud, P. Fiorini, R. Schaijk, and C. Hoof, "Harvesting energy from the motion of human limbs: the design and analysis of an impact based piezoelectric generator", Smart Mater. Struct., Vol. 18, No. 3, pp. 035001, Jan. 2009.

[12] L. Gu and C. Livermore, "Impact-driven, frequency up-converting, coupled vibration energy harvesting device for low frequency operation", Smart Mater. Struct., Vol. 20, No. 4, pp. 045004, Mar. 2011.

[13] Y. Zhang and C. S. Cai, "A retrofitted energy harvester for low frequency vibrations", Smart Mater. Struct., Vol. 21, No. 7, pp. 075007, Jun. 2012.

[14] L. Gu, "Low-frequency piezoelectric energy harvesting prototype suitable for the MEMS implementation", Microelectron. J., Vol. 42, No. 2, pp. 277-282, Feb. 2011.

[15] Q. C. Tang, Y. L. Yang, and X. Li, "Bi-stable frequency up-conversion piezoelectric energy harvester driven by non-contact magnetic repulsion", Smart Mater. Struct., Vol. 20, N0. 12, pp. 125011, Nov. 2011.

[16] I. Sari, T. Balkan, and H. Kulah, "An electromagnetic micro power generator for low-frequency environmental vibrations based on the frequency up conversion technique", J. Microelectromech. Syst., Vol. 19, No. 1, pp. 14-27, Feb. 2010.

[17] T. Galchev, H. Kim, and K. Nazafi, "Micro Power Generator for Harvesting Low-Frequency and Nonperiodic Vibrations", J. Microelectromech. Syst., Vol. 20, No. 4, pp. 852-866, Aug. 2011.

[18] T. Galchev, E. E. Aktakka, and K. Nazafi, "A Piezoelectric Parametric Frequency Increased Generator for Harvesting Low-Frequency Vibrations", J. Microelectromech. Syst., Vol. 21, No. 6, pp. 1311-1320, Dec. 2012.

[19] A. Narimani, M. F. Golnaraghi, and G. N. Jazar, "Frequency response of a piecewise linear vibration isolator", J. Vib. Control, Vol. 10, No. 12, pp. 1775-1794, Dec. 2004.

[20] X. Gao, W. H. Shih and W. Y. Shih, "Induced voltage of piezoelectric unimorph cantilevers of different nonpiezoelectric/piezoelectric length ratios", Smart Mater. Struct., Vol. 18, No. 12, pp. 125018, Dec 2009.

[21] Y. C. Shu and I. C. Lien, "Efficiency of energy conversion for a piezoelectric power harvesting system", J. Micromech. Microeng., Vol. 16, No. 11, pp. 2429-2438, Nov. 2006.